

PERFORMANCE ANALYSIS OF FLAT WINGLET DEFLECTOR ON HYBRID SOLAR PV-WIND TURBINE SYSTEM: CASE STUDY ON TWISTED SAVONIUS TURBINE

Miftah Hijriawan, Zainal Arifin*, Dominicus Danardono Dwi Prija Tjahjana, Ilham Wahyu Kuncoro

Department of Mechanical Engineering, Faculty of Engineering, Universitas Sebelas Maret, Surakarta, Indonesia

* zainal_arifin@staff.uns.ac.id

The harnessing of clean energy from solar and wind constitutes the foremost renewable energy source in Indonesia. The amalgamation of these energy modalities holds the promise of heightened energy efficiency coupled with reduced maintenance expenditures. This investigation endeavors to synergize wind turbines with photovoltaic (PV) solar panels in a hybrid configuration, capitalizing on the turbulent effluent from the wind turbine system as a cooling medium for the solar PV panels. Further studies are needed regarding the Solar PV-Wind Turbine hybrid cooling system, as a system needs to be designed to optimize the direction of airflow from the turbine as a cooling medium for the solar PV panels without compromising the turbine's performance. Experimental-scale modeling is implemented in this study, introducing a flat winglet deflector configuration to refine and optimize the airflow dynamics traversing the turbine, directed towards enhancing the performance of the integrated solar PV-Wind Turbine hybrid system. The results showed that the installation of solar PV panels and the addition of a flat winglet deflector configuration could improve the performance of the turbine. The highest C_p and C_t values obtained were 0.18476 and 0.66404 with an increased value of 21.74% and 20.56% respectively. Using the Taguchi method, the most optimal configuration for C_p is obtained for installing a PV solar panel with a height of 10cm with AoA for installing a flat winglet deflector of 5°. In the ANOVA analysis conducted, it is known that AoA has an effect of up to 71.57%, while the panel height has an effect of 24.69% with an error percentage of 3.73%.

Keywords: solar PV, Savonius, twisted turbine, hybrid system

1 INTRODUCTION

Renewable energy sources still experience many problems in their utilization, one of which is the low efficiency produced due to the limitations of newly developed technology [1]–[4]. This is certainly a challenge for researchers to find the most appropriate solution to overcome these problems. One of the things that can be used to solve this is the integration of hybrid systems to be able to mutually eliminate the shortcomings of each stand-alone system [5], [6]. Because of this, the hybrid system is a promising solution to increase the efficiency of the utilization of renewable energy sources. However, there is a need for investigation regarding the effect of hybrid system integration on each stand-alone system performance.

The utilization of hybrid systems has primarily been confined to augmenting energy output, enhancing overall system efficiency, and optimizing the functional application of said systems [7]–[9]. This phenomenon arises from various factors, including the challenges associated with accurately predicting energy production due to variables such as climate change, weather patterns, and other factors influencing the performance of renewable energy generators. This is particularly pertinent in the case of solar photovoltaic (PV) and wind turbine systems [10]–[12]. For instance, wind energy tends to be more abundant during winter, whereas solar energy availability increases during summer. Furthermore, during nighttime hours when solar energy sources are inactive, wind energy can compensate for this absence, providing a complementary energy source for continuous power generation [13], [14]. In this case, integration between solar PV systems and wind turbines can shorten the investment payback period by up to 2 years and can overcome instability and fluctuations in the power transmission system [15], [16]. Optimizing efficiency in the solar PV-wind turbine hybrid system requires rigorous consideration in selecting an appropriate configuration, encompassing meticulous choices in placement, system layout, and type of turbine.

The integration of wind turbine technology as well as a cooling system in Solar PV can provide a variety of advantages and potential that are quite promising. In this case, the Savonius type Vertical Axis Wind Turbine (VAWT) which has advantages in system simplicity and ease of manufacturing process has good capability to be applied in a hybrid system configuration [17]–[19]. Besides being able to increase the production of energy [20], hybrid integration with a solar PV system can also utilize turbulent exhaust air from a turbine as a cooling medium for solar PV panels. However, there is a need for further studies related to this solar PV-wind turbine hybrid cooling system, this is due to the need to optimize the direction of the airflow passing through the turbine to be used as a direct cooling medium for Solar PV.

Based on research conducted by Wong, Chong, Poh, et al. (2018), who carried out 3D CFD simulations on a vertical axis wind turbine with a flat plate deflector, it was found that under optimal parameter conditions it was able to produce a C_t value 47.10% greater than without using a flat plate deflector. In other experimental and simulation studies, the use of a flat plate deflector for testing H-rotor turbines was able to produce wind speeds 25% greater than the incoming wind [22]. Meanwhile, the research carried out Kuncoro et al. (2023), analysis of the hybrid twisted Savonius

wind turbine and solar PV system shows that the addition of a flat plate deflector is able to increase turbine performance by 10.32%, namely with a C_p value of 0.11678 [23]. In this case, the use of a deflector proved effective in improving both turbine performance and increasing the potential of the wind produced. However, further research is needed regarding the configuration of the deflector to improve the performance and capability of the turbine in a hybrid system with solar PV panels.

In this case, the use of the Savonius type Vertical Axis Wind Turbine (VAWT) technology has the potential as a cooling medium when integrated in a hybrid manner with solar PV because it has a large enough cross-sectional area and can utilize wind energy in various directions (omnidirectional) so that it can optimally circulate air to cool the solar PV panels [24], [25]. By utilizing the drag force of the coming wind [26], The airflow that passes through the turbine blades can be manipulated and then directed to the solar PV panels to improve the cooling process of the system. In addition to the advantages previously described, this solar PV-wind turbine hybrid system still requires identification of placement or additional configuration of each component of the system. In addition to not interfering with the performance of both Solar PV systems and wind turbines [27], it also aims to obtain good cooling performance on Solar PV in order to increase its performance and efficiency. In this case, the PowerNEST configuration which uses a flat winglet deflector can increase wind speed by up to 1.4 times on the surface of the turbine, thereby significantly increasing wind energy output with an increase in power factor reaching 1.7 [28]. This provides the potential to maximize turbine performance while optimizing cooling on exposed solar PV panels.

Considering various issues and previous research, the use of a deflector in the design of a Vertical Axis Wind Turbine (VAWT) system is an intriguing topic for further investigation regarding its impact on the performance of hybrid PV-Wind technology. In this study, the performance of the wind turbine is the primary focus, analyzed to assess its effects through the installation of solar PV panels, incorporating adjustments and designs of flat winglet deflector configurations, taking into account the Angle of Attack. This ensures that the expelled airflow from the wind turbine can be utilized as a cooling system for the PV panels. Additionally, the research aims to analyze the most suitable height positioning between the PV panels and the wind turbine to achieve maximum energy efficiency while minimizing losses.

2 METHOD

2.1 Experimental Setup

This research adapts the PowerNEST system which creates a hybrid system between solar PV and Vertical Axis Wind Turbine (VAWT) configured with a closed frame and equipped with louvers (flat winglet deflectors) [28]. In this case a frame measuring 1.2 m x 1.2 m with a height of 2 m is used as a seat for the helix type Savonius turbine. This type of wind turbine is considered because it has better performance than the ordinary Savonius turbine [15]. This is because the helix-type Savonius turbine rotor has several parts of the surface exposed to the wind at every rotation angle. This generates a continuous positive torque that provides better performance than conventional rotors [29], [30]. The specifications of the Helix-type Savonius turbine used can be seen in Table 1. In addition, on top of the frame is a stand for the placement of solar PV panels which will vary the height distance from the turbine at 5 cm, 10 cm, and 20 cm. At the front of the frame facing the blower is used as a seat for two flat winglet deflectors whose Angle of Attack (AoA) is varied at 5°, 10°, and 15°. The selection of Angle of Attack (AoA) variation is based on the results of a comparison between CFD simulations and experimental testing of the front wing installation in the C15 wind tunnel, where it is known that the optimal Angle of Attack (AoA) ranges from 10° to 20° below the horizontal line [31]. In this case, the selection of AoA below 10° is also analyzed to determine its effect on the air flow to the turbine and the cooling performance of the solar PV panels. The blower here functions to simulate the wind speed coming towards the turbine. The type used is a YAMAMAX brand blower ventilator with a size of 10 inches and a power of 350 watts. 9 units of blowers are used to create enough wind-sweeping area to test the turbine. Blowers are arranged in a 3x3 configuration and placed at a distance of 3 m from the turbine to obtain uniform flow [32]. In more detail, the experimental configuration layout carried out in this study is shown in Figure 1 below.

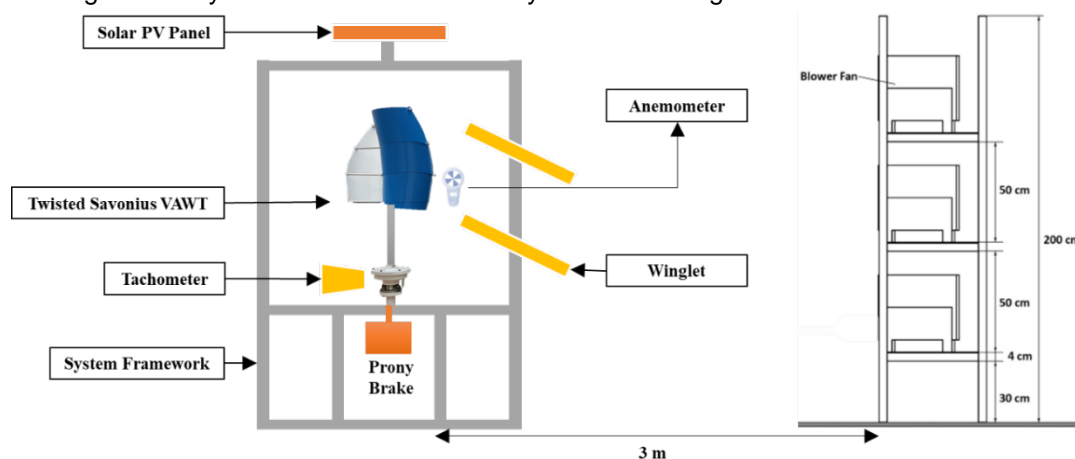


Fig. 1. Experimental research layout configuration

Table 1. Vertical Axis Wind Turbine (VAWT) specifications for the Savonius Helix RC-200SV type [33]

Model	RC-200SV
Start-up Wind Speed	2.5 m/s
Cut-in Wind Speed	3.5 m/s
Rated Wind Speed	12 m/s
Survival Max. wind	45 m/s
Number of Blades	6
Rotor Diameter	0.44 m
Blade Material	Casting aluminum alloy

In the experimental data collection carried out, the wind speed exposed to the turbine was measured at 9 measurement points using an Krisbow Kw06-562 Flexible Thermo Anemometer as shown in Figure 2 below. This was done to obtain the average wind speed in the research experiments carried out. Then the Krisbow KW06-583 digital tachometer is used to measure the rotational speed of the turbine with the measurement point at the base of the turbine shaft. In addition, the Prony brake system is used to determine the torque value of the turbine which is connected using a pulley [34].

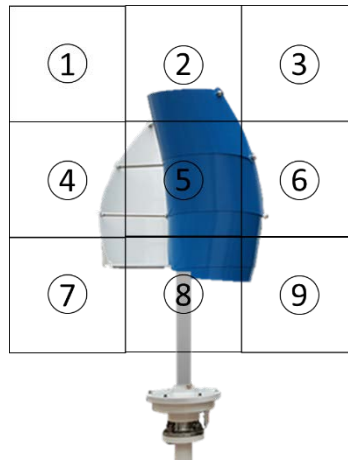


Fig. 2. Schematic of the average wind data collection point

In addition, the Prony brake system is used to determine the torque value of the turbine which is connected using a pulley [34]. In testing the prony brake, 5 load variables were used to get graphs of C_p vs TSR and C_t vs TSR, namely 50 grams, 150 grams, 250 grams, 350 grams, 450 grams and 550 grams. In this case the T_T (torque value, Nm) can be known by Equation (1) [34],

$$T_T = F_e \times R_e \quad (1)$$

Where R_e (effective radius, mm) is determined from the pulley radius plus the rope radius. Meanwhile, F_e (effective forces, N) defined from the Equation (2),

$$F_e = F_s - w \quad (2)$$

In this case, F_s (N) is the reading on a digital scale when the pulley is turned counterclockwise and w (gram) is the weight of the load.

2.2 Performance Analysis

In this study, wind speed exposed to the turbine, turbine rotor rotation, and torque determination using the Prony brake system are the reference data in analyzing the performance of the hybrid system being developed. The theoretical basis of the wind energy conversion system in the Savonius turbine is explained as follows [7], [34], [35]: The potential of available wind energy and exposure to turbine blades in this experiment can be determined by the following Equation (3),

$$P_0 = 1/2\rho AV^3 \quad (3)$$

P_0 is the power available from the wind (Watt), ρ is the density of air (kg/m^3), A is the cross-sectional area of the turbine (m^2), and V is the wind speed (m/s). On the other hand, the power generated from the turbine can be determined by the following Equation (4),

$$P = T \times \omega \quad (4)$$

P is turbine power (Watt), ω is the angular speed (rad/s) and T is the torque value (Nm) which can be known by Equation (5) as follows,

$$T = F_e \times R_e \quad (5)$$

R_e (effective radius) is determined from the pulley radius plus the rope radius (mm). While effective force (F_e) defined from Equation (6) below,

$$F_e = F_s - w \quad (6)$$

F_s is the reading on a digital scale when the pulley is turned counterclockwise (gram) and w is the weight of the load (gram). ω is the angular speed (rad/s) which can be determined with Equation (7) below,

$$\omega = \frac{2\pi N}{60} \quad (7)$$

π is pi (3.14) and N is the rotational speed of the rotor (rpm).

The comparison of the power generated by the turbine (P) with the available wind power (P_o) can be defined as a power coefficient (C_p) with the equation as shown in Equation (8) below,

$$C_p = \frac{T\omega}{\frac{1}{2}\rho AV^3} \quad (8)$$

In addition, the comparison of the actual torque generated by the rotor at a certain wind speed is represented as the torsion coefficient (C_T) can be determined with Equation (9) below,

$$C_T = \frac{C_P}{\lambda} \quad (9)$$

λ is the tip speed ratio (TSR) which can be determined using Equation (10) below,

$$\lambda = \frac{R\omega}{V} = \frac{2\pi NR}{60.V} \quad (10)$$

Where R is the rotor radius (m).

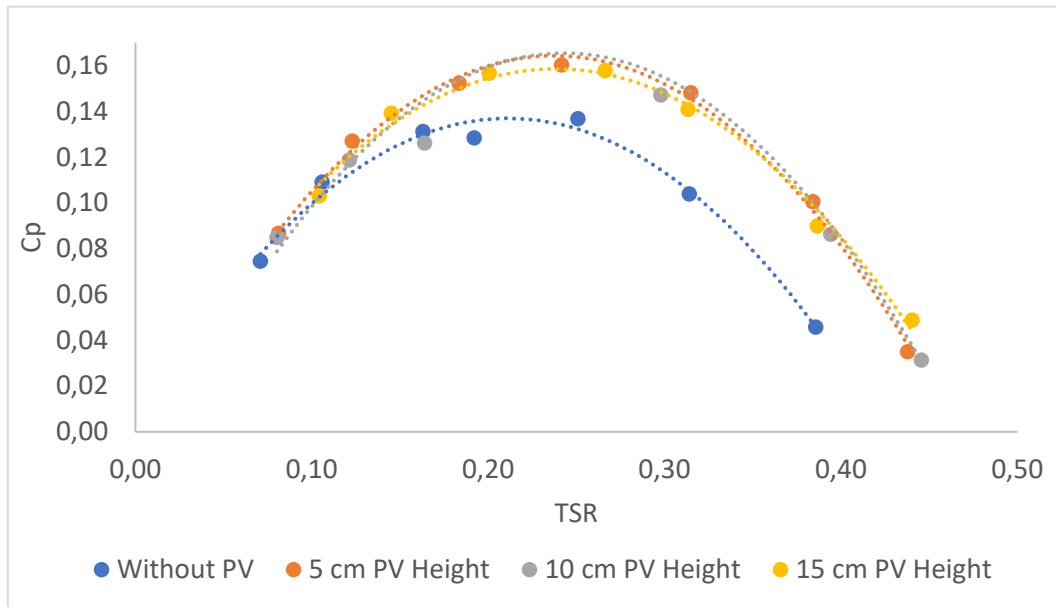
3 RESULT AND DISCUSSION

3.1 Experimental Data Collection

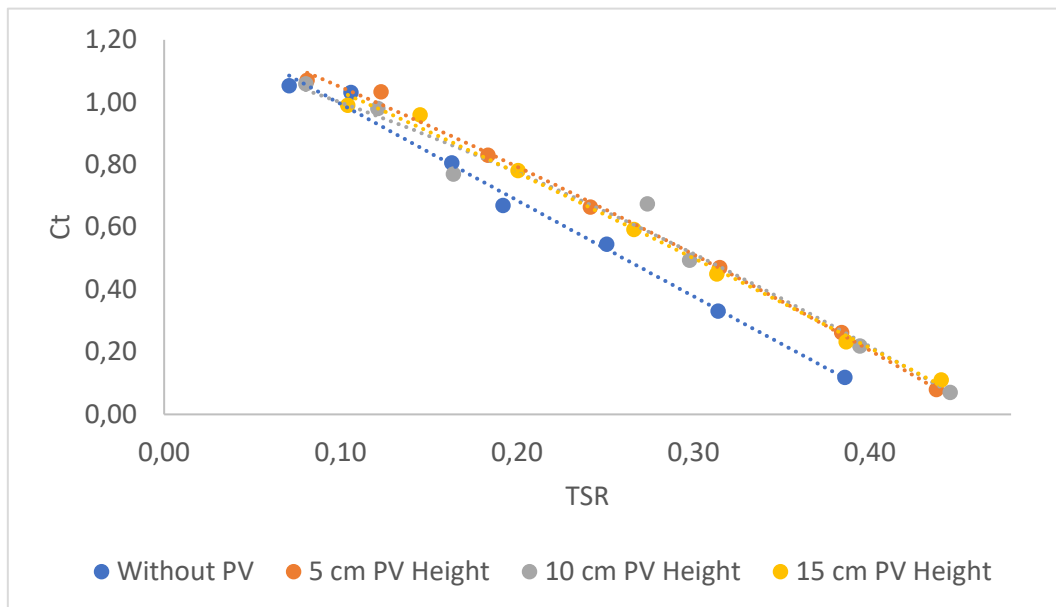
Based on the results of the research experiments that have been carried out, test data were obtained from three variations of the Angle of Attack (AoA) on the installation of the flat winglet deflector, namely 5°, 10°, and 15°. In each AoA variation test, data were obtained for each variation in height from the installation of solar PV panels with a distance of 5 cm, 10 cm, and 15 cm. In collecting data for each AoA variation, the wind speed exposure to the turbine is measured as shown in Figure 2 to determine the average wind speed. Furthermore, turbine rotor rotation speed data and Prony brake readings are used to determine the amount of power produced by the turbine, tip speed ratio (TSR), power coefficient (C_p), and torsion coefficient (C_t) which are further analyzed in each configuration variation. done. In each data collection, it was repeated three times to obtain the average data.

3.2 Turbine Performance on Flat Winglet Deflector Configuration

Based on data collection that has been carried out on variations in the installation of flat winglet deflectors with AoA 5°, it is obtained that the average wind speed that exposes the turbine is 4.81 m/s. There is an increase in average airspeed at each altitude variation that is applied starting from 0.1-0.2 m/s. The highest average airspeed was obtained at a height of 10cm with a speed of 5.04 m/s, while at a height of 15cm, the average airspeed again decreased to 4.86 m/s. In this result also obtained the highest C_p value of 0.18476 at a TSR of 0.27390 which was obtained at the height of the solar PV panel with a distance of 10cm. In addition, the highest C_t value was obtained at 0.67456 which was obtained at the same height. The results of testing with the AoA 5° variation in the form of comparison graphs of C_p vs TSR and C_t vs TSR are shown in Figure 3 below.



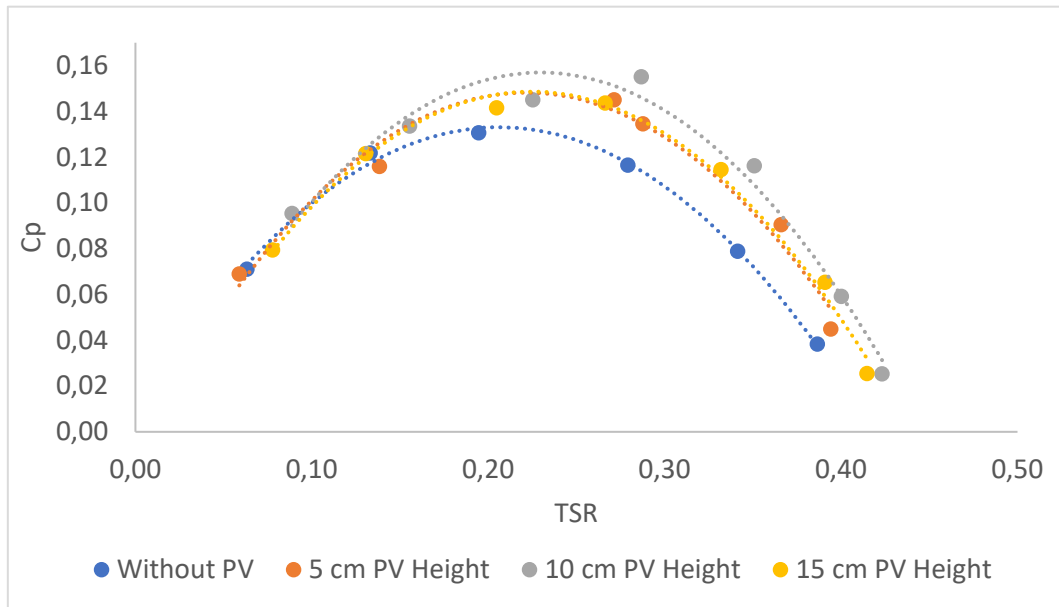
(a)



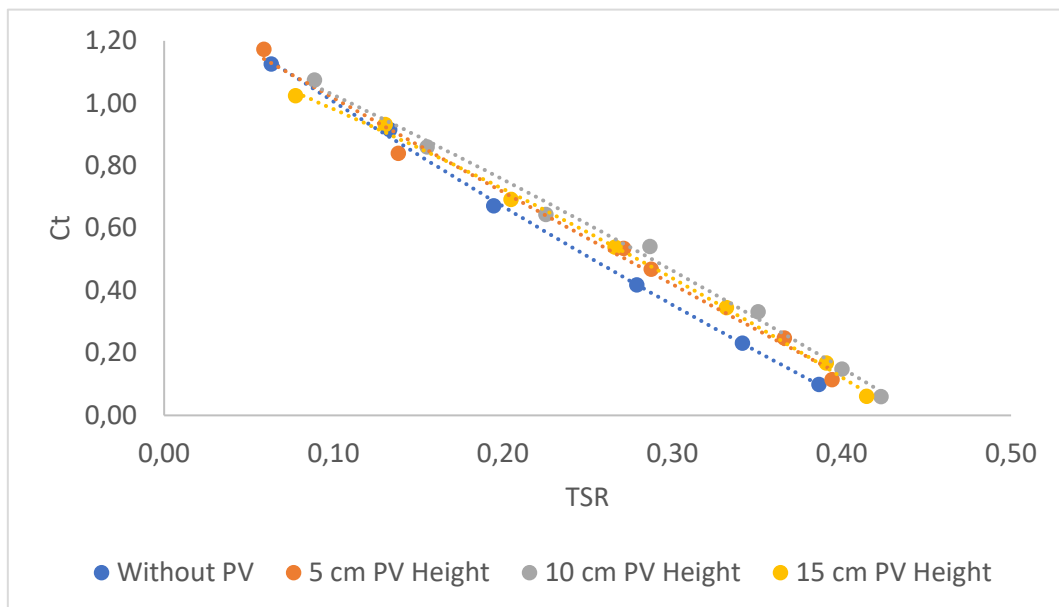
(b)

Fig. 3. The relationship between the height of the PV panel and the turbine system at values (a) C_p vs TSR and (b) C_t vs TSR at AoA 5° Flat Winglet Deflector Configuration

Then in the data collection carried out on variations in the installation of the flat winglet deflector with AoA 10°, the average wind speed value that exposed the turbine was obtained at 4.73 m/s, this has decreased compared to AoA 5° of almost 0.1 m/s. In this result, the highest C_p value was obtained at 0.15513 at a TSR of 0.28670 which was obtained at the height of the solar PV panel with a distance of 10cm. In addition, the highest C_t value was obtained at 0.54110 which was obtained at the same height. The results of testing with a 10° AoA variation in the form of comparison graphs of C_p vs TSR and C_t vs TSR are shown in Figure 4 below.



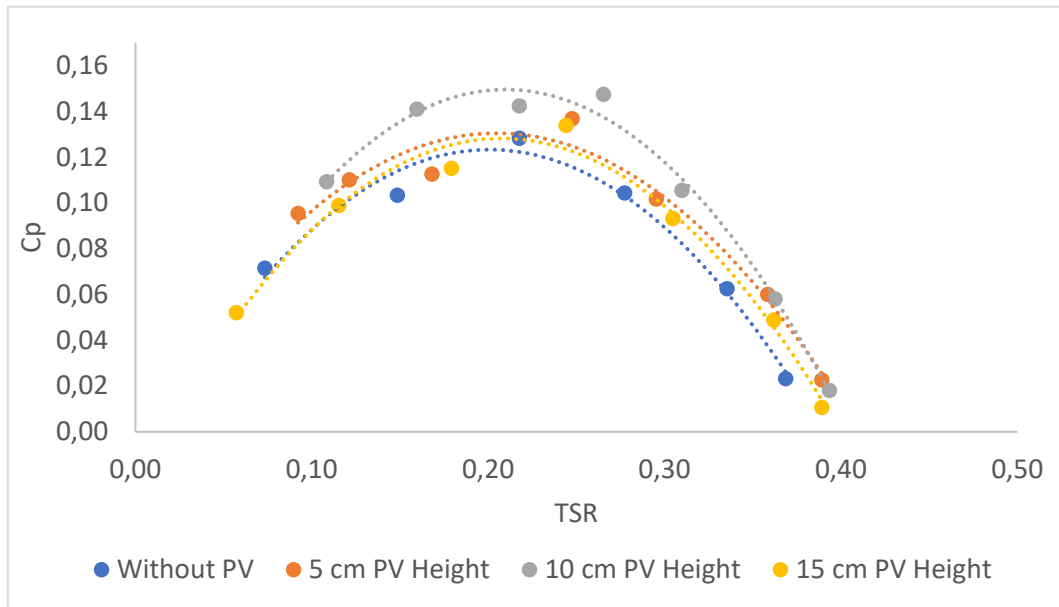
(a)



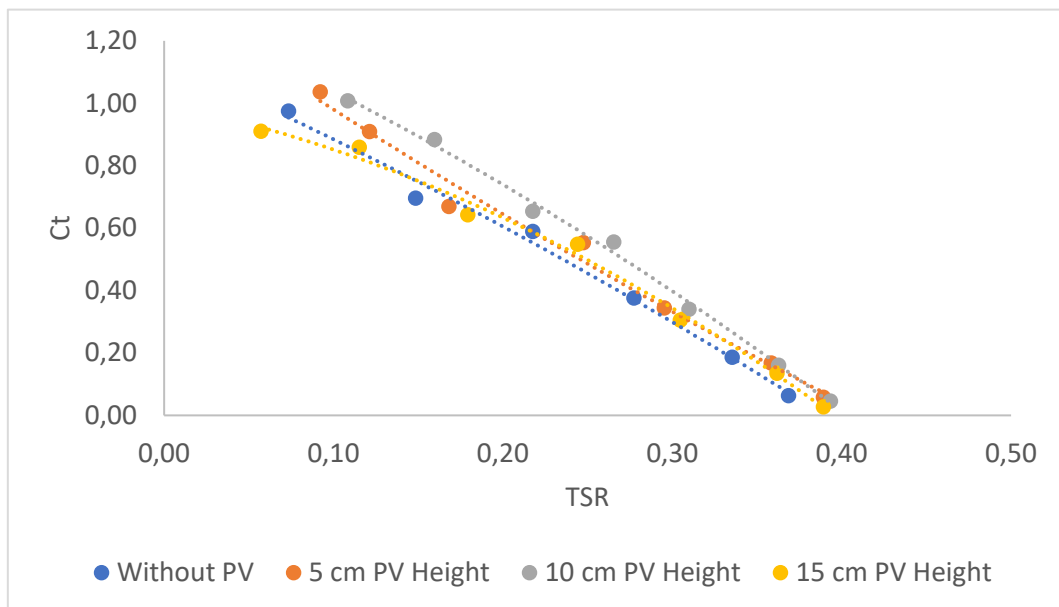
(b)

Fig. 4. The relationship between the height of the PV panel and the turbine system at values (a) C_p vs TSR and (b) C_t vs TSR at AoA 10° Flat Winglet Deflector Configuration

Furthermore, in the data collection carried out on variations in the installation of flat winglet deflectors with AoA 15° , the average wind speed value that exposed the turbine was obtained at 4.62 m/s, this has decreased compared to AoA 5° of almost 0.2 m/s and about 0.1 m/s when compared to AoA 10° . In this result, the highest C_p value was obtained at 0.14745 at a TSR of 0.26537 which was obtained at the height of the solar PV panel with a distance of 10cm. In addition, the highest C_t value was obtained at 0.55566 which was obtained at the same height. The results of the test with the AoA 15° variation in the form of comparison graphs of C_p vs TSR and C_t vs TSR are shown in Figure 5 below.



(a)



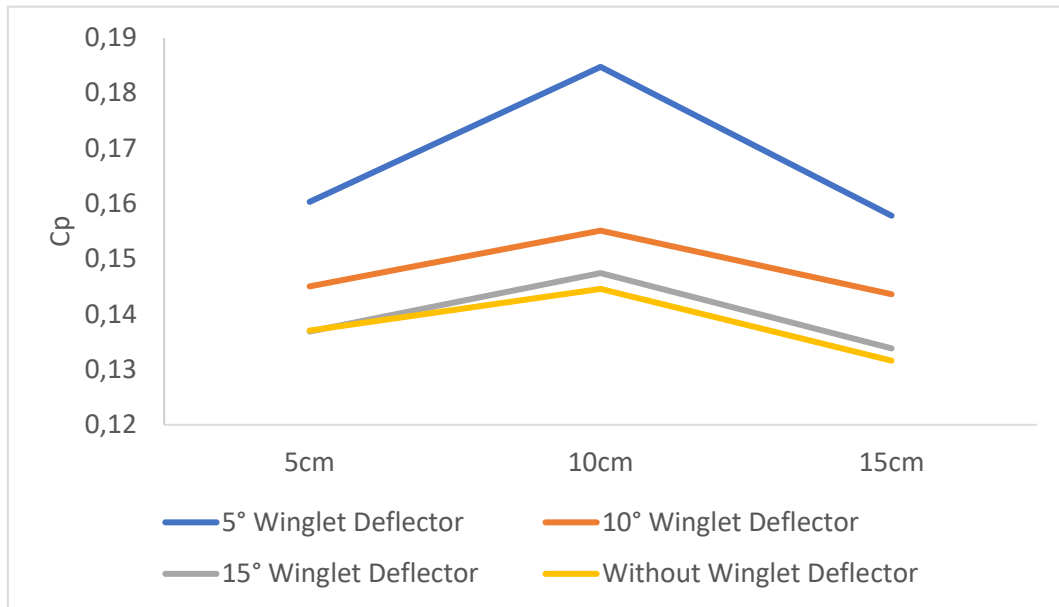
(b)

Fig. 5. The relationship between the height of the PV panel and the turbine system at values (a) C_p vs TSR and (b) C_t vs TSR at $\text{AoA } 15^\circ$ Flat Winglet Deflector Configuration

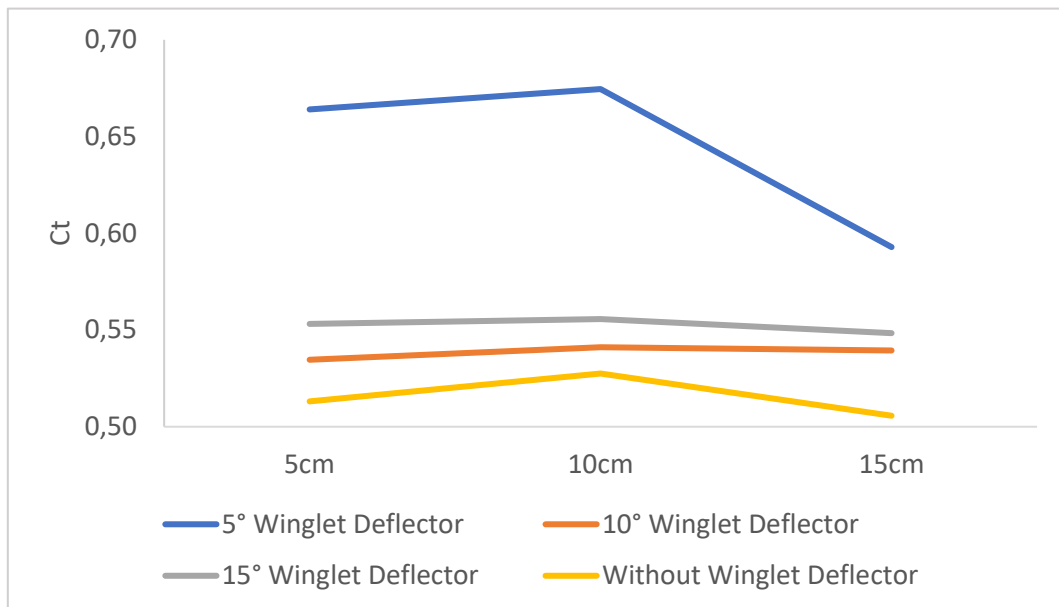
3.3 Turbine Performance Analysis on Hybrid System Configuration

Based on the wind speed measurement data that exposes the turbine, it can be seen that the application of the flat winglet deflector can increase the wind speed by 0.1 m/s to 0.3 m/s. This is due to the venturi effect that occurs due to the installation of the deflector to increase the resulting wind speed [36]–[38], where the highest increase in wind speed was obtained at $\text{AoA } 5^\circ$. In this case, the increase in AoA affects the resulting decrease in wind speed. It can be seen that for every 5° addition to AoA , the wind speed decreases by 0.1–0.2 m/s. The increase in AoA on the flat winglet causes an increase in the induced drag that arises thereby reducing the speed of the air produced [39], [40].

From the data obtained from the three variations of AoA at 5° , 10° , and 15° , it can be seen that the performance of the turbine without installing solar PV panels has the lowest average performance compared to the performance of turbines with installing solar PV panels at various height variations. In this case, the installation of solar PV panels produces an augmented effect such as the endplate of the turbine [41], [42]. The performance comparison graphs on C_p and C_t produced on the bare turbine with each variation are shown in Figure 6 and Table 2 below.



(a)



(b)

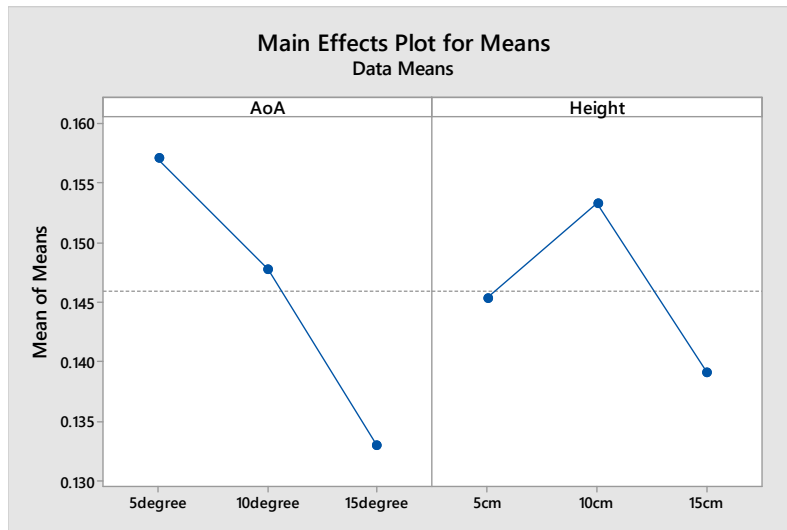
Fig. 6. Performance comparison of the system with the reference (a) C_p and (b) C_t

Table 2. Performance Improvement of Savonius Helix Type Wind Turbine with Flat Winglet Configuration

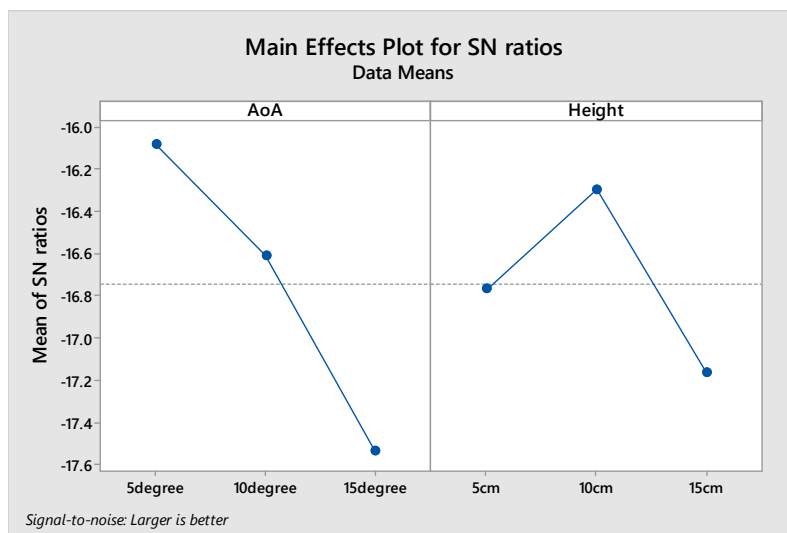
Variation AoA	C_p	Improvement	C_t	Improvement
Bare	0.14459	0.00%	0.52751	0.00%
5°	0.18476	21.74%	0.66404	20.56%
10°	0.15513	6.80%	0.53463	1.33%
15°	0.14745	1.94%	0.55323	4.65%

3.4 Optimum Configuration Analysis

The variation in the height distance of the PV solar panel and the AoA from the installation of the flat winglet deflector influences the value of C_p and C_t produced by the turbine. In this case, the highest C_p value is 0.18476 with an increase of 21.74% which is obtained at the height of the solar PV panel with a distance of 10cm with an AoA variation of 5° and the highest C_t value is 0.66404 with an increase of 20.56% obtained at the same height and variation of AoA. In the resulting C_p analysis, it can be seen that at a height of 10cm solar PV panels with AoA on a flat winglet deflector installation of 5° is the best configuration to produce the most optimal C_p performance based on the results of Taguchi analysis as shown in Figure 7 below.



(a)



(b)

Fig. 7. (a) Main Effects Plot for Mean dan (b) Main Effects for SN ratios of Taguchi Method Analysis

The Analysis of Variance (ANOVA) carried out on each variable tested in the study, shows that each of the variations in the height of the installation of solar PV panels and AoA from the installation of flat winglet deflectors shows significant results, with respective F values of 0.017 and 0.002. On the other hand, the AoA variation shows a greater influence on the results of the research conducted, which is 71.57%, while the height of the solar PV panels shows an effect value of 24.69% with an error value of 3.73% as shown in Table 3 in below.

Table 3. Analysis of Variance

Source	DF	Adj SS	Adj MS	F-Value	P-Value	Contribution
AoA	2	0.000881	0.000440	38.32	0.002	71.5678%
Height	2	0.000304	0.000152	13.22	0.017	24.6954%
Error	4	0.000046	0.000011			3.73679%
Total	8	0.001231				

4 CONCLUSIONS

This study explores the synergistic effects of integrating solar photovoltaic (PV) panels with a Savonius-type helix wind turbine. The investigation includes an analysis of the impact of varying the placement height of solar PV panels and the incorporation of a flat winglet deflector on the system's configuration. The deflector, characterized by different Angle of Attack (AoA) settings, demonstrated notable improvements in turbine performance. The highest attained values for the Coefficient of Power (Cp) and Coefficient of Thrust (Ct) were 0.18476 and 0.66404, respectively,

representing enhancements of 21.74% and 20.56% at a 5° AoA with a panel height of 10cm. The observed performance enhancement is attributed to the solar PV panels acting as an augmented device, similar to an endplate, restricting wind escape at the turbine bucket's end. Consequently, this restriction elevates air pressure, leading to improved turbine performance. Simultaneously, the installation of a flat winglet deflector generates a venturi effect, intensifying the airflow directed towards the turbine. Utilizing the Taguchi method, the optimal configuration for C_p is identified, with a solar PV panel height of 10cm and a 5° AoA for the flat winglet deflector. An analysis of variance (ANOVA) indicates that AoA has a more pronounced influence, contributing 71.57%, while panel height contributes 24.69% to the overall system performance, with an error percentage of 3.73%. From the system modeling that has been conducted, it is expected to become an innovation in hybrid PV-wind technology, which has the potential to be applied on roads by harnessing the wind energy generated by passing vehicles as a driver for vertical wind turbines to create renewable energy.

5 ACKNOWLEDGMENT

This research was supported by a grant from PPS-PTM with the title "Development of a Hybrid Solar PV-Wind Turbine System Configuration Using a Helix Type Savonius Turbine" with contract number 673.1/UN27.22/PT.01.03/2022 from the Ministry of Research, Technology and Higher Education, Republic of Indonesia.

6 REFERENCES

- [1] F. Dong, Y. Li, Y. Gao, J. Zhu, C. Qin, and X. Zhang, "Energy transition and carbon neutrality: Exploring the non-linear impact of renewable energy development on carbon emission efficiency in developed countries," *Resour. Conserv. Recycl.*, vol. 177, no. October 2021, p. 106002, 2022, doi: 10.1016/j.resconrec.2021.106002.
- [2] W. Li, Z. Ji, and F. Dong, "Global renewable energy power generation efficiency evaluation and influencing factors analysis," *Sustain. Prod. Consum.*, vol. 33, pp. 438–453, 2022, doi: 10.1016/j.spc.2022.07.016.
- [3] M. Shalby, A. A. Salah, G. A. Matarneh, A. Marashli, and M. R. Gommaa, "An investigation of a 3D printed micro-wind turbine for residential power production," *Int. J. Renew. Energy Dev.*, vol. 12, no. 3, pp. 550–559, 2023, doi: 10.14710/ijred.2023.52615.
- [4] M. Shalby, A. Abuseif, M. R. Gomaa, A. Marashli, and H. Al-rawashdeh, "Assessment of Dust Properties in Ma' an Wind Farms in Southern," vol. 16, no. 4, pp. 645–652, 2022.
- [5] M. S. Javed, T. Ma, J. Jurasz, and M. Y. Amin, "Solar and wind power generation systems with pumped hydro storage: Review and future perspectives," *Renew. Energy*, vol. 148, pp. 176–192, 2020, doi: 10.1016/j.renene.2019.11.157.
- [6] F. E. Ahmed, R. Hashaikeh, and N. Hilal, "Hybrid technologies: The future of energy efficient desalination – A review," *Desalination*, vol. 495, no. August, p. 114659, 2020, doi: 10.1016/j.desal.2020.114659.
- [7] D. H. Kumar, R. Krishna, M. D. Kumar, R. Pradhan, and M. Sreenivasan, "Harvesting energy from moving vehicles with single-axis solar tracking assisted hybrid wind turbine," *Mater. Today Proc.*, vol. 33, no. xxxx, pp. 326–332, 2020, doi: 10.1016/j.matpr.2020.04.116.
- [8] A. M. Hemeida et al., "Optimum design of hybrid wind/PV energy system for remote area," *Ain Shams Eng. J.*, vol. 11, no. 1, pp. 11–23, 2020, doi: 10.1016/j.asej.2019.08.005.
- [9] X. Xu, W. Hu, D. Cao, Q. Huang, C. Chen, and Z. Chen, "Optimized sizing of a standalone PV-wind-hydropower station with pumped-storage installation hybrid energy system," *Renew. Energy*, vol. 147, pp. 1418–1431, 2020, doi: 10.1016/j.renene.2019.09.099.
- [10] S. Bhattacharjee and S. Acharya, "Performative analysis of an eccentric solar-wind combined system for steady power yield," *Energy Convers. Manag.*, vol. 108, pp. 219–232, 2016, doi: 10.1016/j.enconman.2015.11.023.
- [11] P. Yin, C. Cheng, H. Chen, and T. Wu, "Risk-aware optimal planning for a hybrid wind-solar farm," *Renew. Energy*, vol. 157, pp. 290–302, 2020, doi: 10.1016/j.renene.2020.05.003.
- [12] S. Barakat, H. Ibrahim, and A. A. Elbaset, "Multi-objective optimization of grid-connected PV-wind hybrid system considering reliability, cost, and environmental aspects," *Sustain. Cities Soc.*, vol. 60, no. April, p. 102178, 2020, doi: 10.1016/j.scs.2020.102178.
- [13] M. Talaat, M. A. Farahat, and M. H. Elkholy, "Renewable power integration: Experimental and simulation study to investigate the ability of integrating wave, solar and wind energies," *Energy*, vol. 170, pp. 668–682, 2019, doi: 10.1016/j.energy.2018.12.171.
- [14] K. Doshi and V. S. K. V Harish, "Materials Today: Proceedings Analysis of a wind-PV battery hybrid renewable energy system for a dc microgrid," *Mater. Today Proc.*, no. xxxx, 2020, doi: 10.1016/j.matpr.2020.09.194.
- [15] Y. He, M. Zhang, W. Li, J. Su, and K. Kase, "Feasibility of a new helical blade structure for a PV integrated wind turbine in a heat-driven swirling wind field," *Energy*, vol. 185, pp. 585–598, 2019, doi: 10.1016/j.energy.2019.07.029.

- [16] H. Bakir and A. A. Kulaksiz, "Engineering Science and Technology, an International Journal Modelling and voltage control of the solar-wind hybrid micro-grid with optimized STATCOM using GA and BFA," *Eng. Sci. Technol. an Int. J.*, vol. 23, no. 3, pp. 576–584, 2020, doi: 10.1016/j.jestch.2019.07.009.
- [17] H. Belmili, R. Cheikh, T. Smail, N. Seddaoui, and R. W. Biara, "Study, design and manufacturing of hybrid vertical axis Savonius wind turbine for urban architecture," *Energy Procedia*, vol. 136, pp. 330–335, 2017, doi: 10.1016/j.egypro.2017.10.389.
- [18] A. Vergaerde, T. De Troyer, A. Carbo Molina, L. Standaert, and M. C. Runacres, "Design, manufacturing and validation of a vertical-axis wind turbine setup for wind tunnel tests," *J. Wind Eng. Ind. Aerodyn.*, vol. 193, no. March, 2019, doi: 10.1016/j.jweia.2019.103949.
- [19] B. Hand and A. Cashman, "A review on the historical development of the lift-type vertical axis wind turbine: From onshore to off shore floating application," *Sustain. Energy Technol. Assessments*, vol. 38, no. January, 2020, doi: 10.1016/j.seta.2020.100646.
- [20] F. A. Khan, N. Pal, and S. H. Saeed, "Review of solar photovoltaic and wind hybrid energy systems for sizing strategies optimization techniques and cost analysis methodologies," *Renewable and Sustainable Energy Reviews*, vol. 92. Elsevier Ltd, pp. 937–947, Sep. 2018. doi: 10.1016/j.rser.2018.04.107.
- [21] K. H. Wong, W. T. Chong, S. C. Poh, Y. C. Shiah, N. L. Sukiman, and C. T. Wang, "3D CFD simulation and parametric study of a flat plate deflector for vertical axis wind turbine," *Renew. Energy*, vol. 129, pp. 32–55, Dec. 2018, doi: 10.1016/J.RENENE.2018.05.085.
- [22] K. H. Wong *et al.*, "Experimental and simulation investigation into the effects of a flat plate deflector on vertical axis wind turbine," *Energy Convers. Manag.*, vol. 160, no. January, pp. 109–125, 2018, doi: 10.1016/j.enconman.2018.01.029.
- [23] I. W. Kuncoro, Z. Arifin, E. P. Budiana, and M. Hijriawan, "Improvement Performance Twisted Savonius Wind Turbine on Hybrid System: Effect of Flat Plate Deflector Installation," *Int. J. Heat Technol.*, vol. 41, no. 3, pp. 742–748, 2023, doi: 10.18280/ijht.410330.
- [24] N. Korprasertsak and T. Leephakpreeda, "Analysis and optimal design of wind boosters for Vertical Axis Wind Turbines at low wind speed," *J. Wind Eng. Ind. Aerodyn.*, vol. 159, no. October, pp. 9–18, 2016, doi: 10.1016/j.jweia.2016.10.007.
- [25] C. J. Bai and W. C. Wang, "Review of computational and experimental approaches to analysis of aerodynamic performance in horizontal-axis wind turbines (HAWTs)," *Renew. Sustain. Energy Rev.*, vol. 63, pp. 506–519, 2016, doi: 10.1016/j.rser.2016.05.078.
- [26] G. Abdalrahman, W. Melek, and F. S. Lien, "Pitch angle control for a small-scale Darrieus vertical axis wind turbine with straight blades (H-Type VAWT)," *Renew. Energy*, vol. 114, pp. 1353–1362, 2017, doi: 10.1016/j.renene.2017.07.068.
- [27] E. Pinheiro, F. Bandejas, M. Gomes, P. Coelho, and J. Fernandes, "Performance analysis of wind generators and PV systems in industrial small-scale applications," *Renew. Sustain. Energy Rev.*, vol. 110, no. December 2018, pp. 392–401, 2019, doi: 10.1016/j.rser.2019.04.074.
- [28] B. Patankar, R. Tyagi, D. Kiss, and A. B. Suma, "Evaluation of an Integrated Roof Wind Energy System for urban environments," *J. Phys. Conf. Ser.*, vol. 753, no. 10, 2016, doi: 10.1088/1742-6596/753/10/102007.
- [29] A. Damak, Z. Driss, and M. S. Abid, "Experimental investigation of helical Savonius rotor with a twist of 180°," *Renew. Energy*, vol. 52, pp. 136–142, 2013, doi: 10.1016/j.renene.2012.10.043.
- [30] Z. Zhao, Y. Zheng, X. Xu, W. Liu, and G. Hu, "Research on the improvement of the performance of savonius rotor based on numerical study," *2009 Int. Conf. Sustain. Power Gener. Supply*, pp. 1–6, 2009, doi: 10.1109/SUPERGEN.2009.5348197.
- [31] J.-J. Tan, P. Myler, and W.-A. Tan, "Investigation and Analysis on Racing Car Front Wings," *DEStech Trans. Eng. Technol. Res.*, 2017, doi: 10.12783/dtetr/mdm2016/4896.
- [32] W. T. Chong *et al.*, "Cross axis wind turbine: Pushing the limit of wind turbine technology with complementary design," *Appl. Energy*, vol. 207, pp. 78–95, 2017, doi: 10.1016/j.apenergy.2017.06.099.
- [33] REXCO, "RC-200SV-46," 2020. <http://www.bestwindsolar.com/product/RC-200SV-46.html> (accessed Dec. 25, 2020).
- [34] D. D. P. Tjahjana, Z. Arifin, S. Suyitno, W. E. Juwana, A. R. Prabowo, and C. Harsito, "Experimental study of the effect of slotted blades on the Savonius wind turbine performance," *Theor. Appl. Mech. Lett.*, vol. 11, no. 3, p. 100249, 2021, doi: 10.1016/j.taml.2021.100249.
- [35] K. Rogowski and R. Maroński, "CFD computation of the savonius rotor," *J. Theor. Appl. Mech.*, vol. 53, no. 1, pp. 37–45, 2015, doi: 10.15632/jtam-pl.53.1.37.
- [36] S. Das Karmakar and H. Chattopadhyay, "A review of augmentation methods to enhance the performance of vertical axis wind turbine," *Sustain. Energy Technol. Assessments*, vol. 53, no. PA, p. 102469, 2022, doi: 10.1016/j.seta.2022.102469.

- [37] A. Hesami, A. H. Nikseresht, and M. H. Mohamed, "Feasibility study of twin-rotor Savonius wind turbine incorporated with a wind-lens," *Ocean Eng.*, vol. 247, no. January, p. 110654, 2022, doi: 10.1016/j.oceaneng.2022.110654.
- [38] B. A. Storti, J. J. Dorella, N. D. Roman, I. Peralta, and A. E. Albanesi, "Improving the efficiency of a Savonius wind turbine by designing a set of deflector plates with a metamodel-based optimization approach," *Energy*, vol. 186, p. 115814, 2019, doi: 10.1016/j.energy.2019.07.144.
- [39] G. A. A. Thuwis, R. De Breuker, M. M. Abdalla, and Z. Gürdal, "Aeroelastic tailoring using lamination parameters :Drag reduction of a Formula One rear wing," *Struct. Multidiscip. Optim.*, vol. 41, no. 4, pp. 637–646, 2010, doi: 10.1007/s00158-009-0437-6.
- [40] S. Ganesan and B. Esakki, "Computational fluid dynamic analysis of an unmanned amphibious aerial vehicle for drag reduction," *Int. J. Intell. Unmanned Syst.*, vol. 8, no. 3, pp. 187–200, 2020, doi: 10.1108/IJIUS-01-2019-0003.
- [41] A. S. Saad, I. I. El-Sharkawy, S. Ookawara, and M. Ahmed, "Performance enhancement of twisted-bladed Savonius vertical axis wind turbines," *Energy Convers. Manag.*, vol. 209, p. 112673, Apr. 2020, doi: 10.1016/j.enconman.2020.112673.
- [42] A. S. Saad, A. Elwardany, I. I. El-Sharkawy, S. Ookawara, and M. Ahmed, "Performance evaluation of a novel vertical axis wind turbine using twisted blades in multi-stage Savonius rotors," *Energy Convers. Manag.*, vol. 235, p. 114013, May 2021, doi: 10.1016/J.ENCONMAN.2021.114013.

Paper submitted: 31.05.2023.

Paper accepted: 09.02.2024.

This is an open access article distributed under the CC BY 4.0 terms and conditions